



Synchronization of reaction–diffusion Hopfield neural networks with s-delays through sliding mode control*

Xiao Liang^{a,1} , Shuo Wang^a  Ruili Wang^b 
Xingzhi Hu^c , Zhen Wang^a 

^aSchool of Mathematics and System Science,
Shandong University of Science and Technology,
Qingdao, China, 266590
mathlx@163.com

^bInstitute of Applied Physics and Computational Mathematics,
Beijing, China, 100094

^cChina Aerodynamics Research and Development Center,
Mianyang, China, 621000

Received: November 4, 2020 / **Revised:** July 24, 2021 / **Published online:** January 17, 2022

Abstract. Synchronization of reaction–diffusion Hopfield neural networks with s-delays via sliding mode control (SMC) is investigated in this paper. To begin with, the system is studied in an abstract Hilbert space $C([-r, 0], U)$ rather than usual Euclid space \mathbb{R}^n . Then we prove that the state vector of the drive system synchronizes to that of the response system on the switching surface, which relies on equivalent control. Furthermore, we prove that switching surface is the sliding mode area under SMC. Moreover, SMC controller can also force with any initial state to reach the switching surface within finite time, and the approximating time estimate is given explicitly. These criteria are easy to check and have less restrictions, so they can provide solid theoretical guidance for practical design in the future. Three different novel Lyapunov–Krasovskii functionals are used in corresponding proofs. Meanwhile, some inequalities such as Young inequality, Cauchy inequality, Poincaré inequality, Hanalay inequality are applied in these proofs. Finally, an example is given to illustrate the availability of our theoretical result, and the simulation is also carried out based on Runge–Kutta–Chebyshev method through Matlab.

Keywords: distributed system, sliding mode control, synchronization, Lyapunov–Krasovskii functional, s-delay.

*The work was supported by the National Numerical Wind-Tunnel (grant No. NNW2019ZT7-A13), Challenge Project (grant No. TZ2018001), Development Program for Defense Department of China (grant No. C1520110002), and Natural Science Foundation of Shandong Province (grant No. ZR2021MA056).

¹Corresponding author.

1 Introduction

Hopfield neural networks (HNNs) are intensively studied since it was first postulated in [10] due to their successful applications in numerous areas such as pattern recognition, parallel computation, and associative memory [22]. The original version of the model is described by ODEs, which is just an approximation of real world. Several factors are neglected in this model.

To begin with, the delay is inevitably encountered in electronic implementation of neural networks (NNs) due to finite speed of switching and transmission of signals [8, 21] or deliberately introduced to deal with moving image processing [27]. It is necessary to incorporate distributed delays into the system when the NNs usually have a spatial extent due to presence of a multitude of parallel pathways with a variety of axon sizes and lengths [27]. After a scrutiny scan of published work on delayed HNNs, we find that most authors either concentrate on system with discrete delays or distributed delays independently. However, in the real signal propagation, we often encounter the case that NNs possess both discrete and distributed delays at the same time. From the viewpoint of mathematics, s -delays is an accurate and suitable tool to describe discrete and distributed delays at once since both of them can be included in the s -delays [9]. It has the form $\int_{-\tau_i}^0 f_i(u_i(t+s)) d\kappa_i(s)$, where f_i , $i = 1, 2, \dots, n$, are activation functions, $\kappa_i(s)$ are Lebesgue–Stieljies measurable functions. So if we study the HNNs with s -delays, it means that our model is more general than the previous model.

On the other hand, diffusion phenomenon is also neglected in the original model of HNNs. Actually, diffusion effect cannot be ignored in NNs when electrons move in an inhomogeneous electromagnetic field [14, 16]. Reaction–diffusion Hopfield neural networks (RDHNNs) not only have theoretical influence, but also have been used in numerous frontier regions such as image encryption [32], pattern formation [40]. Compared with original HNNs, RDHNNs are described through partial differential equations with initial and boundary conditions. It not only involves the time variable, but also the space variables.

Based on above discussion, the model will be more exact if we study the diffusion phenomenon and delay effect simultaneously. However, it is worth noting that delay is a source of oscillation, bifurcation, and instability, which hinders the practical application of HNNs [8, 14, 21]. Meanwhile, diffusion can also harm the stability of the system [14, 16]. The dynamical behavior of HNNs will be even more complex when incorporating these two factors.

As an important collective behavior, synchronization of HNNs becomes a hot topic in recent decades due to their potential applications in secure communications, signal processing, distributed computation [7, 11, 17, 18, 28, 30, 31, 35, 36, 42]. It means that solution of drive system converges to the desired trajectory under appropriate control strategy [26]. However, synchronization of HNNs is still not fully conducted because it is hard to guide the solution so that it converges to ideal trajectory due to their complexity. This situation will be even worse if we take both reaction–diffusion phenomenon and s -delays into consideration.

Many effective strategies have been proposed for the synchronization of HNNs with either delay or reaction diffusion term. For example, the point-wise and optimal control

by [31], pinning control by [17, 30], intermittent control by [7, 11, 18], impulse control by [28, 36, 42], nonlinear feedback control by [6]. It should be pointed out that these strategies heavily rely on Schur complement theorem, and in these papers, the criteria is free reaction–diffusion coefficients.

SMC is considered as a potential approach in synchronization of HNNs, which is a discontinuous control. Its main advantages are fast response, good transient performance, and robustness to external disturbance [1, 19, 23, 25, 29, 33, 34]. A great volume of the literature has been published on the theory and application of SMC for various systems [25, 33]. As to HNNs, [22] has pointed out the importance of sliding mode in recurrent neural networks, especially, how to prevent sliding. [29] investigates the synchronization of uncertain nonidentical chaotic neural networks with time delays via SMC. To the best of our knowledge, there is still no existing result on synchronization of delayed reaction–diffusion Hopfield neural networks via SMC until yet, let alone with s -delays.

Motivated by above discussion, synchronization of reaction–diffusion HNNs with s -delays is studied in this paper. Challenges and difficulties will be confronted since numerous factors are taken into account in this model. To begin with, both reaction–diffusion term and s -delay are considered in the model, and the delay is more general than previous ones. Moreover, reaction–diffusion term is an extension of Laplace operator Δ . At last, we have checked the published work of SMC for distributed systems, there is still no simulation on the motion of equivalent control and SMC controller versus time and space.

Compared to some previously published results, our results are less conservative, and the model is more general. Main contributions are summarized as follows.

- (i) Choosing appropriate Hilbert space $C([-r, 0], U)$ for state variables is a critical step toward analyzing and approximating it. In the previous work of delayed reaction–diffusion HNNs, phase space is chosen to be the usual Euclidean space \mathbb{R}^n . The structure of \mathbb{R}^n is simple, concrete, and easy to grasp. However, the theoretical result is richer in abstract Hilbert space $C([-r, 0], U)$ than that in \mathbb{R}^n , and the form of the system is much more concise in Hilbert space.
- (ii) SMC is successfully applied for the synchronization of this system. It is reliable and easy to be programmed and operated on the computer. Both sliding mode equation and control law are established by using the equivalent control. This is different from the previous work in SMC of other distribution systems, which use matrix splitting technique [19, 23, 34] or direct design of discontinuous control law [24, 25].
- (iii) There is no existing specialized software suited for synchronization of reaction–diffusion Hopfield neural networks with s -delays. In order to accomplish these goals, we discrete this system and write the code by ourselves. Then simulation is obtained via Matlab to validate the efficiency of our result.
- (iv) The proofs of main theorems are based on constructing appropriate Lyapunov–Krasovskii functionals (LKFs). Meanwhile, some inequalities such as Young inequality, Hanalay inequality are used in the process. These criteria are expressed in the matrix norm, which are also easy to check. These criteria are also explicitly expressed when compared with LMIs.

2 Preliminaries and notations

We list some notations, which will be used in the following sections.

- For $A \in \mathbb{R}^{n \times n}$, $A \geq 0$ means A is a semipositive definite matrix;
- E is the identity matrix of $\mathbb{R}^{n \times n}$;
- $A \circ B = (a_{ij}b_{ij})_{n \times n}$ is the Hadamard product between $A \in \mathbb{R}^{n \times n}$ and $B \in \mathbb{R}^{n \times n}$ [20];
- $L^2(\mathcal{O})$ denotes the space of square integrable functions on \mathcal{O} ;
- $U = \{L^2(\mathcal{O})\}^n$, it becomes a Hilbert space when equipped with the usual inner product (u, v) , $u, v \in U$, and the corresponding norm is $\|u\| = \sqrt{(u, u)}$;
- $C([-r, 0], U)$ is the Banach space of all continuous functionals from $[-r, 0]$ to U with the supnorm $\|\varphi\|_C = \sup_{-r \leq s \leq 0} \|\varphi(s)\|$;
- $u_t(s) = u(t + s)$ for $s \in [-r, 0]$;
- tr is the trace operator;
- $\|A\|_F = \sqrt{\text{tr}(A^T A)}$ is called the Frobenius norm of $A \in \mathbb{R}^{m \times n}$ [20].

The drive system of reaction diffusion HNNs with s-delays is

$$\begin{aligned} \frac{\partial u}{\partial t} &= \nabla \cdot (D(x) \circ \nabla u) - Au + Cf \left(\int_{-r}^0 u(t + s, x) \, d\eta(s) \right) + I + Pv, \\ \frac{\partial u}{\partial \nu}(t, x) &= 0, \quad t \geq 0, \quad x \in \partial\mathcal{O}, \\ u(s, x) &= \phi(s, x), \quad s \in [-r, 0], \end{aligned} \tag{1}$$

where n is the number of neurons, $u = (u_1, u_2, \dots, u_n)^T$ is the state vector. T denotes the transpose of matrix. $\mathcal{O} \subset \mathbb{R}^l$ is a connected bounded set with smooth boundary $\partial\mathcal{O}$. Gradient operator of u is $\nabla u = (\nabla u_1, \nabla u_2, \dots, \nabla u_n)^T$, where $\nabla u_i = (\partial u_i / \partial x_1, \partial u_i / \partial x_2, \dots, \partial u_i / \partial x_l)^T$, $i = 1, 2, \dots, n$. $f(u) = (f_1(u_1), f_2(u_2), \dots, f_n(u_n))^T$ is a diagonal map with f_i , $i = 1, 2, \dots, n$, represent activation function, $A = \text{diag}(a_1, a_2, \dots, a_n)$ is the rate matrix with $a_i > 0$. $C = (c_{ij})_{n \times n}$ is weights matrix. $I = (I_1, I_2, \dots, I_n)^T$ is bias vector. $\phi(s, x) = (\phi_1(s, x), \phi_2(s, x), \dots, \phi_n(s, x))^T$ is the initial function, which is continuous in $[-r, 0] \times \mathcal{O}$, r is time delay, $D(x) = (D_{ij}(x))_{n \times l}$ is diffusion coefficient matrix, which is determined by Fick's law [14]. Let $Y = (y_{ij})_{n \times l} = D \circ \nabla u = (D_{ij} \partial u_i / \partial x_j)_{n \times l}$ is the Hadamard product of matrix D and ∇u . $Y = (Y_1, Y_2, \dots, Y_n)^T$, $\nabla \cdot Y$ is the general divergence operator of matrix Y , which is defined as $\nabla \cdot Y = (\nabla \cdot Y_1, \nabla \cdot Y_2, \dots, \nabla \cdot Y_n)^T$. $\nabla \cdot Y_i$ is the divergence operator of vector Y_i . $\partial u / \partial \nu = (\partial u_1 / \partial \nu, \partial u_2 / \partial \nu, \dots, \partial u_n / \partial \nu)^T$, $\partial u_i / \partial \nu = (\partial u_i / \partial x_1, \partial u_i / \partial x_2, \dots, \partial u_i / \partial x_m)^T$. Adiabatic boundary condition is used in this article.

S-delays are defined through the Lebesgue–Stieljies integral as $\int_{-r}^0 u(t + s, x) \, d\eta(s) = (\int_{-r}^0 u_1(t + s, x) \, d\eta_1(s), \dots, \int_{-r}^0 u_n(t + s, x) \, d\eta_n(s))^T$. $\eta_i(s)$ are nondecreasing functions with bounded variation. In other words, there exist positive constants q_i such that $\int_{-r}^0 d\eta_i(s) = q_i < \infty$. v is the control strategy on drive system. P is the dimensionless control matrix, which is to be determined.

The response system of reaction diffusion HNNs with s-delays is

$$\begin{aligned} \frac{\partial u_r}{\partial t} &= \nabla \cdot (D(x) \circ \nabla u_r) - Au_r + Cf \left(\int_{-r}^0 u_r(t+s, x) d\eta(s) \right) + I, \\ \frac{\partial u_r}{\partial \nu}(t, x) &= 0, \quad t \geq 0, x \in \partial\mathcal{O}, \\ u_r(s, x) &= \psi(s, x), \quad s \in [-r, 0], \end{aligned} \quad (2)$$

with $u_r = (u_r^1, u_r^2, \dots, u_r^n)^T$, $\psi(s, x) = (\psi_1(s, x), \psi_2(s, x), \dots, \psi_n(s, x))^T$ is also continuous on $[-r, 0] \times \mathcal{O}$. Other symbols have the same physical meaning as those in (1).

The tracking vector error $e(t, x)$ is defined as the difference between the observed behavior of the drive system (1) and its desired behavior of response system (2), which means

$$e(t, x) = u(t, x) - u_r(t, x). \quad (3)$$

From (1)–(3) we have

$$\begin{aligned} \frac{\partial e}{\partial t} &= \nabla \cdot (D(x) \circ \nabla e) - Ae + Cf \left(\int_{-r}^0 u(t+s, x) d\eta(s) \right), \\ &\quad - Cf \left(\int_{-r}^0 u_r(t+s, x) d\eta(s) \right) + Pv, \\ \frac{\partial e}{\partial \nu}(t, x) &= 0, \quad t \geq 0, x \in \partial\mathcal{O}, \\ e(s, x) &= \varpi(s, x), \quad x \in \mathcal{O}, s \in [-r, 0], \end{aligned} \quad (4)$$

where $\varpi = \phi(s, x) - \psi(s, x)$.

Remark 1. Let

$$\eta_i(s) = \begin{cases} 0, & -r \leq s < 0, \\ 1, & s = 0, \end{cases}$$

where $i = 1, 2, \dots, n$. Then, through calculating the Lebesgue–Stieljies integral, the governing equation of (1) is transformed to

$$\frac{\partial u}{\partial t} = \nabla \cdot (D(x) \circ \nabla u) - Au + Cf(u(t-r, x)) + I + Pv.$$

This is the system with discrete delay.

If there exists the function $\kappa(s)$ such that $d\eta(s) = \kappa(s) ds$, then calculating the Lebesgue–Stieljies integral, the governing equation of (1) is reduced to

$$\frac{\partial u}{\partial t} = \nabla \cdot (D(x) \circ \nabla u) - Au + Cf \left(\int_{-r}^0 u(t+s, x) \kappa(s) ds \right) + I + Pv.$$

This is the system with distributed delays.

2.1 Tracking error in the Banach space

Let us define the diffusion operator as

$$\mathfrak{A} : \mathcal{D}(\mathfrak{A}) \in U \rightarrow U, \quad \mathfrak{A}e = \nabla \cdot (D(x) \circ \nabla e), \quad e \in \mathcal{D}(\mathfrak{A}), \tag{5}$$

and $\mathcal{D}(\mathfrak{A})$ is the domain of \mathfrak{A} , which is defined as [14]

$$\mathcal{D}(\mathfrak{A}) = \left\{ e : e \in \{H^2(\mathcal{O})\}^n, \frac{\partial e}{\partial \nu} \Big|_{\partial \mathcal{O}} = 0 \right\}.$$

Define the Nemytskii operator as follows [14]:

$$f(e)(x) = f(e(x)), \quad x \in \mathcal{O}.$$

Then (4) is equivalent to the following functional differential equation in Hilbert space $C([-r, 0], U)$:

$$\begin{aligned} \frac{de}{dt} &= Pv + \mathfrak{A}e - Ae + C\tilde{f}, \\ e(s) &= \varpi(s), \quad \varpi \in C([-r, 0], U), \end{aligned} \tag{6}$$

where

$$\tilde{f} = f\left(\int_{-r}^0 u(t+s) d\eta(s)\right) - f\left(\int_{-r}^0 u_r(t+s) d\eta(s)\right).$$

In this paper, we assume

(H1) $|f_i(u_i) - f_i(v_i)| \leq \sigma_i |u_i - v_i|$ for all $u_i, v_i \in \mathbb{R}$;

(H2) There exist two positive constants α, β such that $\alpha \leq D_{ij}(x) \leq \beta$.

Definition 1. The drive system (1) and response system (2) are said to be exponentially synchronized under appropriate controller v if there are constants $\mu > 0$ and $\iota > 0$ such that

$$\|e\| \leq \|\varpi\|_C \exp\{-\iota t\}, \quad t > 0,$$

where e is defined in (3) and (6).

Let us construct a new matrix $\tilde{M} = (\tilde{m}_{ij})_{n \times n}$ based on $M = (m_{ij})_{n \times n}$ with $\tilde{m}_{ii} = m_{ii}\alpha$, and $\tilde{m}_{ij} = -|m_{ij}|\beta, i \neq j$. Then we have

Lemma 1. If (H2) holds and \tilde{M} is a M -matrix, then $(u, M\mathfrak{A}u) \leq 0, u \in U$.

Proof. We first prove the following equality by using the property of Hadmard product, and the basic relationship $\nabla \cdot (u_i Y_i) = u_i \nabla \cdot Y_i + \langle \nabla u_i, Y_i \rangle$, and $\langle \cdot, \cdot \rangle$ denotes the standard inner product of Euclid space \mathbb{R}^l , then we have

$$\nabla \cdot (XMY) = \nabla \cdot \left(\sum_{j=1}^n m_{1j} u_j Y_j, \sum_{j=1}^n m_{2j} u_j Y_j, \dots, \sum_{j=1}^n m_{nj} u_j Y_j \right)^T$$

$$\begin{aligned}
 &= \left(\sum_{j=1}^n m_{1j} u_j \nabla \cdot Y_j + \sum_{j=1}^n m_{1j} \langle \nabla u_j, Y_j \rangle, \dots, \right. \\
 &\quad \left. \sum_{j=1}^n m_{nj} u_j \nabla \cdot Y_j + \sum_{j=1}^n m_{nj} \langle \nabla u_j, Y_j \rangle \right)^T \\
 &= XM\nabla Y + \begin{pmatrix} m_{11} & m_{12} & \dots & m_{1n} \\ m_{21} & m_{22} & \dots & m_{2n} \\ \dots & \dots & \dots & \dots \\ m_{n1} & m_{n2} & \dots & m_{nn} \end{pmatrix} \begin{pmatrix} \langle \nabla u_1, Y_1 \rangle \\ \langle \nabla u_2, Y_2 \rangle \\ \dots \\ \langle \nabla u_n, Y_n \rangle \end{pmatrix},
 \end{aligned}$$

where $X = \text{diag}(u_1, u_2, \dots, u_n)$.

Furthermore

$$\begin{pmatrix} \langle \nabla u_1, Y_1 \rangle \\ \langle \nabla u_2, Y_2 \rangle \\ \dots \\ \langle \nabla u_n, Y_n \rangle \end{pmatrix} = \begin{pmatrix} \frac{\partial u_1}{\partial x_1} y_{11} + \dots + \frac{\partial u_1}{\partial x_l} y_{1l} \\ \frac{\partial u_2}{\partial x_1} y_{21} + \dots + \frac{\partial u_2}{\partial x_l} y_{2l} \\ \dots \\ \frac{\partial u_n}{\partial x_1} y_{n1} + \dots + \frac{\partial u_n}{\partial x_l} y_{nl} \end{pmatrix} = (\nabla u \circ Y)J, \tag{7}$$

where $J = (1, 1, \dots, 1)^T$, which means

$$\nabla \cdot (XMY) = XM\nabla Y + M(\nabla u \circ Y)J. \tag{8}$$

In other words, we have

$$XM\nabla Y = \nabla \cdot (XMY) - M(\nabla u \circ Y)J. \tag{9}$$

Let $Y=D(x)\circ\nabla u$ in (9), and use the general Gauss formula for the matrix

$$\begin{aligned}
 \int_{\mathcal{O}} \nabla \cdot Z \, dx &= \int_{\mathcal{O}} \nabla \cdot (Z_1, Z_2, \dots, Z_n)^T \, dx \\
 &= \left(\int_{\mathcal{O}} \nabla \cdot Z_1 \, dx, \int_{\mathcal{O}} \nabla \cdot Z_2 \, dx, \dots, \int_{\mathcal{O}} \nabla \cdot Z_n \, dx \right)^T \\
 &= \left(\int_{\partial\mathcal{O}} Z_1 \, ds, \int_{\partial\mathcal{O}} Z_2 \, ds, \dots, \int_{\partial\mathcal{O}} Z_n \, ds \right)^T \\
 &= \int_{\partial\mathcal{O}} (Z_1, Z_2, \dots, Z_n)^T \, ds = \int_{\partial\mathcal{O}} Z \, ds,
 \end{aligned}$$

where Z_i is the i th column of Z . By using the adiabatic boundary condition we have

$$\begin{aligned}
 &\int_{\mathcal{O}} XM\nabla \cdot (D(x) \circ \nabla u) \, dx \\
 &= \int_{\mathcal{O}} \nabla \cdot XM(D(x) \circ \nabla u) \, dx - \int_{\mathcal{O}} M(\nabla u \circ (D(x) \circ \nabla u))J \, dx
 \end{aligned}$$

$$\begin{aligned}
&= \int_{\partial\mathcal{O}} XM(D(x) \circ \nabla u) \, dx - \int_{\mathcal{O}} M(\nabla u \circ (D(x) \circ \nabla u))J \, dx \\
&= - \int_{\mathcal{O}} M(\nabla u \circ (D(x) \circ \nabla u))J \, dx.
\end{aligned} \tag{10}$$

Then using (H2), (9)–(10), Cauchy inequality $(u, v) \leq \|u\|\|v\|$, and $(u, u) = \|u\|^2$, we have

$$\begin{aligned}
(e, M\mathfrak{A}e) &= - \int_{\mathcal{O}} \sum_{i=1}^n \sum_{j=1}^n m_{ij} \langle \nabla u_i, D_j \circ \nabla u_j \rangle \, dx \\
&\leq - \int_{\mathcal{O}} \sum_{i=1}^n m_{ii} \langle \nabla u_i, D_i \circ \nabla u_i \rangle \, dx - \int_{\mathcal{O}} \sum_{i \neq j} m_{ij} \langle \nabla u_i, D_j \circ \nabla u_j \rangle \, dx \\
&\leq -(u^+)^T \widetilde{M} u^+,
\end{aligned} \tag{11}$$

where $u^+ = (\|\nabla u_1\|, \|\nabla u_2\|, \dots, \|\nabla u_n\|)^T$. Since \widetilde{M} is a M-matrix, then we have

$$(e, M\mathfrak{A}e) \leq 0. \tag{12}$$

The proof is complete. \square

3 Sliding mode equation

In this work, switching surface is defined as a linear combination of the current states

$$s_0 = \{e: S(e, t) = Ke = 0\}, \tag{13}$$

where K satisfies $\det(KP) \neq 0$, which will be determined later.

According to the SMC theory, when the system trajectories reach onto the switching surface, it follows that $dS/dt = 0$. In other words,

$$K \frac{de}{dt} = 0. \tag{14}$$

By substituting (6) into (14) we get

$$K P v + K \mathfrak{A} e - K A e + K C \tilde{f} = 0 \tag{15}$$

with the assumption that KP is invertible, we obtain the equivalent control

$$v_{\text{eq}} = -\widetilde{B}\mathfrak{A}e + \widetilde{B}Ae - \widetilde{B}C\tilde{f} \tag{16}$$

with $\widetilde{B} = (KP)^{-1}K$.

By substituting v_{eq} into (6) we get the sliding mode

$$\begin{aligned} \frac{de}{dt} &= (E - B)\mathfrak{A}e - (E - B)Ae + (E - B)C\tilde{f}, \\ e(s) &= \varpi(s), \quad s \in [-r, 0], \end{aligned} \quad (17)$$

where $B = P\tilde{B} = P(KP)^{-1}K$. We also assume that $M \triangleq E - B$ is invertible throughout this article.

For the convenience of study, we rewrite system (17) as follows:

$$\begin{aligned} \frac{de}{dt} &= M\mathfrak{A}e - Ae + BAe + MC\tilde{f}, \\ e(s) &= \varpi(s), \quad s \in [-r, 0]. \end{aligned} \quad (18)$$

We have the following main theorem of this article.

Theorem 1. *If system (6) satisfies (H1)–(H2) and*

$$\begin{aligned} \text{(H3)} \quad a_m - n\gamma^{-1}\|MC\|_F^2\sigma_M^2q^2 &> 0, \quad a_m = \min\{a_1, a_2, \dots, a_n\}, \\ \sigma_M &= \max\{\sigma_1, \sigma_2, \dots, \sigma_n\}, \quad \gamma = a_m > 0, \quad q = \max\{q_1, q_2, \dots, q_n\}, \end{aligned}$$

A and B is exchangeable, then the state vector of the drive system synchronizes to that of the response system on the sliding surface (13).

Proof. Let us define the Lyapunov–Krasovskii functional as follows:

$$V(e_t) = \|e_t(0)\|^2. \quad (19)$$

The derivative of $V(e_t)$ with respect to t along any trajectory of system (18) is given by

$$\begin{aligned} \frac{d}{dt}V(e) &= 2\left(\frac{de}{dt}, e\right) \\ &= 2(M\mathfrak{A}e, e) - 2(Ae, e) + 2(BAe, e) + 2(MC\tilde{f}, e). \end{aligned} \quad (20)$$

By Lemma 1 we have

$$(e, M\mathfrak{A}e) < 0. \quad (21)$$

By the positiveness of diagonal entries of A we have

$$-2(e, Ae) \leq -2a_m\|e\|^2, \quad (22)$$

where $a_m = \min\{a_1, a_2, \dots, a_n\}$.

By using $B = P(KP)^{-1}K$, $Ke = 0$ in the sliding mode (18), the exchangeable assumption, we get

$$2(BAe, e) = 0. \quad (23)$$

By Young inequality, $\|\Psi e\| \leq \sqrt{n}\|\Psi\|_F\|e\|$ [14], the definition of \tilde{f} , where f is a diagonal map, condition (H1), and total boundedness of Lebesgue–Stieljies integral $\int_{-r}^0 d\eta_i(s) = q_i < \infty$ we have

$$\begin{aligned} (e(t), MC\tilde{f}) &\leq \frac{1}{2}\gamma\|e\|^2 + \frac{1}{2}\gamma^{-1}\|MC\tilde{f}\|^2 \leq \frac{1}{2}\gamma\|e\|^2 + \frac{1}{2}\gamma^{-1}n\|MC\|_F^2\|\tilde{f}\|^2 \\ &\leq \frac{1}{2}\gamma\|e\|^2 + \frac{1}{2}\gamma^{-1}n\|MC\|_F^2\sigma_M^2q^2 \sup_{s \in [-r,0]} \|et + s\|^2 \\ &\leq \frac{1}{2}\gamma\|e\|^2 + \frac{1}{2}\gamma^{-1}n\|MC\|_F^2\sigma_M^2q^2\|e_t\|_C^2. \end{aligned} \quad (24)$$

In this case, we choose $\gamma = a_m$. By (19)–(24) we have

$$\frac{dV}{dt} \leq -\gamma V + c_1 \sup_{s \in [-r,0]} V(t+s)$$

with $c_1 = na_m^{-1}\|MC\|_F^2\sigma_M^2q^2$.

By the Hanalay inequality we have $V(t) \leq \|\varpi\|_C \exp\{-(\gamma - c_1)t\}$. By (H3) we have $\gamma > c_1$.

So the solution of (6) is exponentially stable on the sliding mode described by (18). By Definition 1 the drive system (1) and the response system (2) are synchronized in (13). \square

Remark 2. After a scrutiny scan of the latest works of synchronization for delayed or reaction–diffusion HNNs [2, 4, 7, 11, 12, 17, 18, 30, 37–40], we find that these criteria are expressed in the form of LMI toolbox, which heavily rely on the Schur complement theorem and optimization method. Compared with them, our criteria based on matrix norm are expressed explicitly. But their method is also an efficient tool, especially, when the uncertain disturbance is also taken into consideration [3, 4, 37, 40]. One of our object is to apply the LMIs techniques for this subject. Furthermore, our method is similar to the integral inequality method used in [41] and interval matrix method used in [36]. Although their criteria have wide range in application, the model in [41] and [36] is belong to an ordinary differential equation, only time variable is considered. We still hope their methods can be extended to our model in the future work. By the way, the previous criteria for synchronization of reaction–diffusion HNNs are free reaction coefficients D_{ij} [7, 11, 17, 18, 28, 40]. But reaction coefficients is incorporated into our result through (H2) and (H3).

4 Sliding mode area

Theorem 2. Consider system (6) with assumptions (H1)–(H3). Suppose that the switching surface is given by (13), the SMC law is designed to be

$$v(x, t) = v_{\text{eq}} - \varepsilon \frac{(KP)^{-1}S}{\|Be\|^2}, \quad \varepsilon > 0, \quad (25)$$

where $v_{\text{eq}} = -B\mathfrak{A}e + BAe - BC\tilde{f}$, ε is a positive scalar, which will be selected properly. Then switching surface s_0 is the sliding mode area under (25).

Proof. Consider the Lyapunov–Krasovskii functional as follows:

$$V(t) = \frac{1}{2} \|S\|^2. \quad (26)$$

Using (13), the derivative of (26) with respect to time is given as follows:

$$\frac{d}{dt} V = \int_{\mathcal{O}} S^T \frac{\partial S(x, t)}{\partial t} dx = \int_{\mathcal{O}} e^T K^T K (\mathfrak{A}e - Ae + C\tilde{f} + Pv) dx.$$

By substituting SMC controller (25) into above equation we have

$$\begin{aligned} \frac{d}{dt} V &= \int_{\mathcal{O}} e^T K^T K \left(\mathfrak{A}e - Ae + C\tilde{f} + P \left(v_{\text{eq}} - \varepsilon \frac{(KP)^{-1}S}{\|Be\|^2} \right) \right) dx \\ &= \int_{\mathcal{O}} e^T K^T KM (\mathfrak{A}e - Ae + C\tilde{f}) dx \\ &\quad - \int_{\mathcal{O}} \varepsilon e^T K^T KP (KP)^{-1} \frac{Ke}{\|Be\|^2} dx. \end{aligned}$$

Since

$$KB = KP(KP)^{-1}K = K, \quad BP = P(KP)^{-1}KP = P,$$

we have

$$e^T K^T KM = e^T K^T K(E - B) = e^T K^T (K - KB) = 0.$$

Then

$$\begin{aligned} \frac{d}{dt} V &= - \int_{\mathcal{O}} \varepsilon e^T K^T KP (KP)^{-1} \frac{Ke}{\|Be\|^2} dx \\ &= -\varepsilon \int_{\mathcal{O}} \frac{S^T S}{\|Be\|^2} dx = -\varepsilon \frac{\|S\|^2}{\|Be\|^2}. \end{aligned}$$

We finally get

$$\frac{d}{dt} V < 0 \quad \text{if } S \neq 0,$$

which means that any trajectory of (6) can be driven to remain on the sliding surface under SMC controller (25). \square

Remark 3. As we all know, chattering cannot be eliminated in the SMC. It is one of the shortages associated with this method. If we replace (25) with

$$v = v_{\text{eq}} - \varepsilon \frac{(KP)^{-1}S}{\|Be\|^2 + \delta}, \quad \varepsilon > 0, \delta > 0,$$

the SMC controller becomes continuous, then chattering will disappear. However, the total robustness of SMC also will be lost correspondingly if continuation is utilized. So the reasonable strategy is to reduce rather than remove chattering in the future study.

5 Approximate time to the sliding manifolds

Theorem 3. *If the SMC law is chosen as (25), it can be shown that the reachability of the switching surface s_0 is guaranteed, and the reaching time T_r satisfies*

$$T_r = \frac{1}{2}\varepsilon^{-1}\|P(KP)^{-1}K\varpi\|^2. \quad (27)$$

Proof. Let us construct the Lyapunov–Krasovskii functional as follows:

$$V(t) = \frac{1}{2}\|Be_t(0)\|^2. \quad (28)$$

By using (25) the derivative of V with respect to t is given as follows:

$$\begin{aligned} \frac{d}{dt}V &= - \int_{\mathcal{O}} e^T B^T B \frac{\partial e}{\partial t} dx \\ &= \int_{\mathcal{O}} e^T B^T B (\mathfrak{A}e - Ae + C\tilde{f} + Pv) dx \\ &= \int_{\mathcal{O}} e^T B^T (B^2 - B) (\mathfrak{A}e - Ae + C\tilde{f}) dx - \varepsilon \int_{\mathcal{O}} e^T B^T BP \frac{(KP)^{-1}Be}{\|Be\|^2} dx. \end{aligned}$$

By using

$$B^2 = (P(KP)^{-1}K)^2 = B, \quad BP = P, \quad KB = K, \quad B = P\tilde{B}$$

we have

$$\frac{d}{dt}V = -\varepsilon \int_{\mathcal{O}} \frac{(Be)^T Be}{\|Be\|^2} dx = -\varepsilon.$$

We suppose that the trajectory of (6) will reach s_0 at time T_r , and by definition of $S(e)$, which means $S(e(T_r)) = 0$,

$$\|Be(T_r)\|^2 - \|Be(0)\|^2 = -2\varepsilon T_r.$$

So

$$T_r = \frac{1}{2}\varepsilon^{-1}\|P(KP)^{-1}K\varpi\|^2. \quad (29)$$

In other words, the SMC law (25) can drive error system (6) to the switching surface s_0 in finite time T_r . \square

Remark 4. It can be seen from Theorems 1 and 3 that control law based on equivalent control is efficient for the target studied in this paper. The construction of control law is very tricky, and the method is direct. This is different from the previous work in SMC for other distribution systems, which use matrix splitting technique [19, 23, 34] or direct design of discontinuous control law [24, 25]. Their methods are suitable for those system, which is difficult to build equivalent control and can be utilized to deal with complex model. We will attempt to apply those methods to our system in the future study.

6 Example and simulation

In this example,

$$u = (u_1, u_2)^T, \quad u_r = (u_r^1, u_r^2)^T, \quad U = \{L^2(\mathcal{O})\}^2, \\ \phi = (\cos(0.2\pi x), \cos(0.2\pi x))^T, \quad \psi = (3 \cos(0.2\pi x), -2 \cos(0.2\pi x))^T.$$

Both of them are continuous in $[-1, 0] \times \mathcal{O}$, and

$$\varpi = \phi - \psi = (2 \cos(0.2\pi x), -3 \cos(0.2\pi x))^T.$$

$r = 1$ and

$$\eta_1(s) = \eta_2(s) = \begin{cases} 0, & -1 \leq s < 0, \\ 1, & s = 0. \end{cases} \tag{30}$$

Through calculating Leabesgue–Stieljies integral, we get

$$\int_{-1}^0 u_i(t + s, x) \, d\eta(s) = u_i(t - 1, x), \quad i = 1, 2.$$

We also have $\int_{-1}^0 d\eta_i(s) = 1$ by calculation. $q_1 = q_2 = 1$ are selected in this case.

Moreover, $f_1(u_1) = \tanh(u_1)$, $f_2(u_2) = \tanh(u_2)$, so f is a diagonal map. Since $|\tanh(x) - \tanh(y)| < |x - y|$, $x, y \in \mathbb{R}$, so $f_1(u_1)$, $f_2(u_2)$ are global Lipschitz continuous functions with $\sigma_1 = 1$, $\sigma_2 = 1$, and $\sigma_M = 1$. So (H1) is satisfied. We also have

$$A = \begin{bmatrix} 4 & 0 \\ 0 & 4 \end{bmatrix}, \quad C = \begin{bmatrix} 0.5 & -0.2 \\ -5 & 0.5 \end{bmatrix}, \quad I = \begin{bmatrix} 5 \\ 2 \end{bmatrix}, \quad P = \begin{bmatrix} 0.1 \\ 0.2 \end{bmatrix},$$

$D_1(x) = 1$, $D_2(x) = 1$ such that $\nabla \cdot (D_1(x)\nabla u_1) = \Delta u_1$, $\nabla \cdot (D_2(x)\nabla u_2) = \Delta u_2$, Δ is a Laplacian operator.

The simulation is carried out through Matlab. The code is based on the finite difference method. Specifically, the second-order centered difference scheme is utilized to discrete the space. The Runge–Kutta–Chebyshev method is used to discrete the time. We use this scheme to simulate the dynamical behavior of uncontrolled part of drive system. For detailed information, please see Figs. 1–2. From Fig. 1 the surface of response system is very complicated, especially, it seems that there is no equilibrium for u_r . It is unstable for them. To give a clear description of it, we also simulate the frequency of u_r in Fig. 1, which coincides with Fig. 1.

We also design

$$K = (1, 2), \quad PK = \begin{bmatrix} 0.1 & 0.2 \\ 0.2 & 0.4 \end{bmatrix}, \quad KP = 0.5,$$

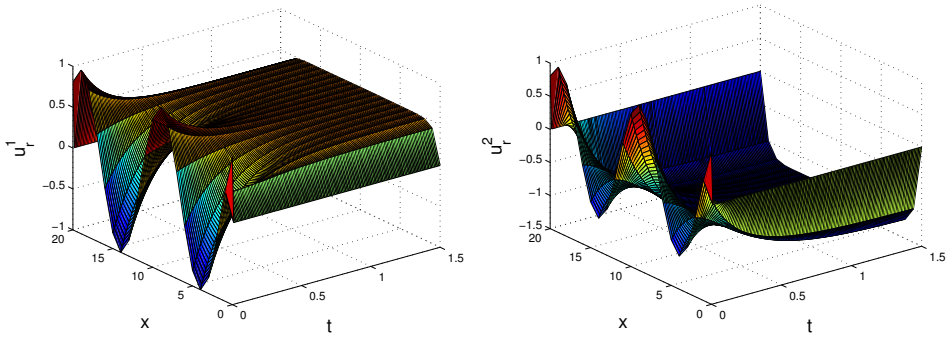


Figure 1. Simulation of u_r^1 (left) and u_r^2 (right) in response system.

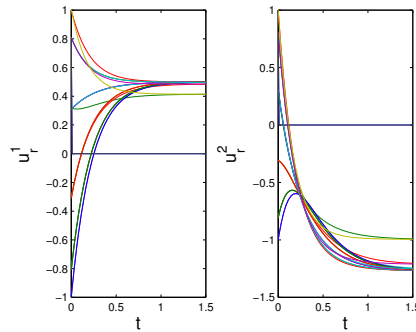


Figure 2. Frequency of u_r^1 (left) and u_r^2 (right) in response system.

then

$$\begin{aligned} \tilde{B} &= (KP)^{-1}K = (2, 4), & B &= P(KP)^{-1}K = \begin{bmatrix} 0.2 & 0.4 \\ 0.4 & 0.8 \end{bmatrix}, \\ M &= E - B = \begin{bmatrix} 0.8 & -0.4 \\ -0.4 & 0.2 \end{bmatrix}. \end{aligned}$$

Since $\alpha = \beta = 1$ is chosen, then $\tilde{M} = M$ is the semipositive definite matrix,

$$MC = \begin{bmatrix} 2.4 & -0.36 \\ -1.2 & 0.18 \end{bmatrix}, \quad \|MC\|_F = 7.3620.$$

This means $a_m - na_m^{-1}\|MC\|_F^2\sigma_M^2q^2 = 0.3190 > 0$. So (H3) is fulfilled. By Theorem 1 the behavior of (2) synchronizes to (1) in the switching surface $s_0 = \{e: e_1 + 2e_2 = 0\}$.

According to (16), the equivalent control is

$$\begin{aligned} v_{eq} &= 2\Delta e_1 + 4\Delta e_2 - 2e_1 - 4e_2 \\ &\quad + 19(\tanh(u_1(t-1)) - \tanh(u_r^1(t-1))) \\ &\quad - 1.6(\tanh(u_2(t-1)) - \tanh(u_r^2(t-1))). \end{aligned}$$

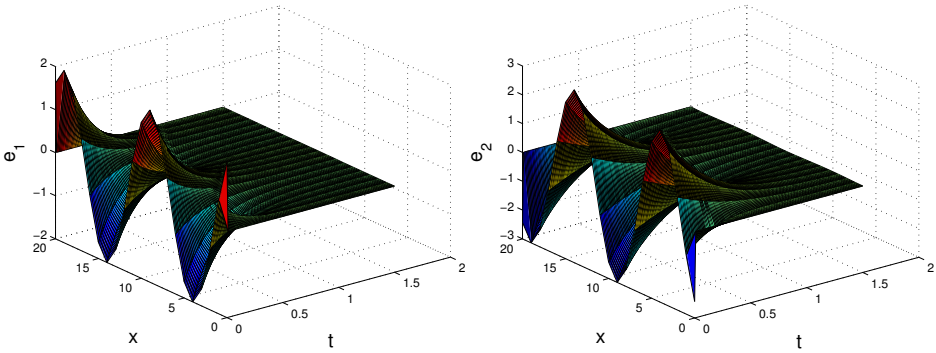


Figure 3. Simulation of e_1 (left) and e_2 (right) in error system.

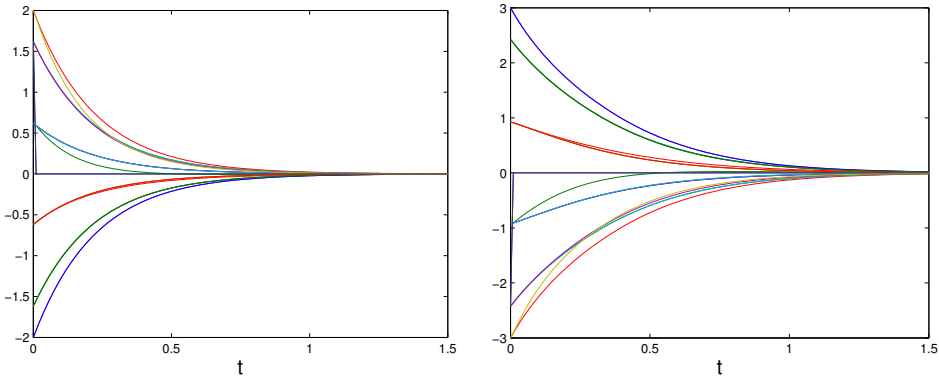


Figure 4. Frequency of e_1 (left) and e_2 (right) in error system under SMC.

Furthermore, the SMC is defined as

$$v = v_{eq} - \frac{8e_1 + 16e_2}{\int_0^{20} (e_1 + e_2)^2 dx}$$

when $\varepsilon = 1$.

Figure 3 presents the asymptotic behavior for error system. The reason why we choose 3-D plot is that it is visual and intuitive. We can check the evolution of the system not only from the time span, but also from the space span. We can see that as time t increases to the infinity, the error surfaces of e_1 and e_2 converge to the equilibrium 0 in the sliding manifold. It coincides with the result of Theorem 1.

To present a more clear information of e_1, e_2 , we also give the trajectory of e_1, e_2 for some chosen x in Fig. 4, which coincides with Fig. 3.

We also give the simulation of equivalent control v_{eq} and SMC v in Fig. 5. We can see that v is slightly enhanced versus time to drive the error dynamics e into the equilibrium 0.

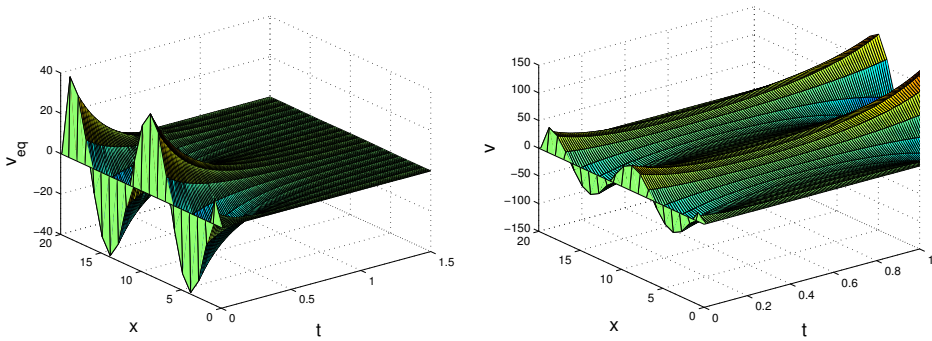


Figure 5. Simulation of equivalent control v_{eq} (left) and SMC v (right).

7 Conclusion and discussion

This paper focuses on theoretical analysis of synchronization for reaction–diffusion Hopfield neural networks with s -delays, which is a prerequisite step for practical design of NNs. SMC is used in this process. Namely, linear switching surface is constructed and equivalent control involving delay and diffusion term is obtained in the Hilbert space $C([-r, 0], U)$. SMC is designed based on the equivalent control. We find that state vector of error system converges to the switching surface in finite time. Approximate time and sliding mode area is obtained by using the LKFs. Moreover, the exponential stability of solution on the switching surface is also obtained by using Lyapunov–Krasovskii functional. These LKFs are different. Last, we provide an example to show the availability of our method, and the corresponding simulation is also given by using the Matlab. We can find that SMC v is enhanced versus time to ensure the ideal property of controlled system.

SMC is still a promising field. Many different strategies have been proposed for SMC. For instance, integral sliding surface is a reasonable alternative for linear sliding surface. Unfortunately, after a scrutiny scan into published results on SMC for distributed systems, we find that the linear sliding surface is still the only option in selecting switching surface due to its distinct structure [1, 13, 19, 25]. So exploiting nonlinear sliding surface is one of our research direction in the future. The splitting technique will also be discussed for the design of SMC for distributed systems in the future work [19]. By the way, the noise is unavoidable in the real world [14, 15], so synchronization of stochastic reaction diffusion HNNs with s -delays will be considered in the next work. LMIs are also potential tools in the synchronization of this system, which are easy to be examined through Matlab toolbox by finding feasible solutions [5].

Acknowledgment. We would like to acknowledge our debt to the rigorous editors and preminent reviewers. The paper is dramatically improved after following their constructive suggestions and detailed comments.

References

1. Y. Cao, J. Lam, Robust H_∞ control of uncertain Markovian jump systems with time-delay, *IEEE Trans. Autom. Control*, **45**(1):77–83, 2000, <https://doi.org/10.1109/9.827358>.
2. Y. Cao, R. Samidurai, R. Sriraman, Robust passivity analysis for uncertain neural networks with leakage delay and additive time-varying delays by using general activation function, *Math. Comput. Simul.*, **155**:57–77, 2019, <https://doi.org/10.1016/j.matcom.2017.10.016>.
3. Y. Cao, R. Samidurai, R. Sriraman, Stability and dissipativity analysis for neutral type stochastic Markovian jump static neural networks with time delays, *J. Artif. Intell. Soft Comput. Res.*, **9**(3):189–204, 2019, <https://doi.org/10.2478/jaiscr-2019-0003>.
4. Y. Cao, R. Sriraman, N. Shyamsundarraj, R. Samidurai, Robust stability of uncertain stochastic complex-valued neural networks with additive time-varying delays, *Math. Comput. Simul.*, **171**:207–220, 2020, <https://doi.org/10.1016/j.matcom.2019.05.011>.
5. H. Choi, LMI-based sliding surface design for integral sliding mode control of mismatched uncertain systems, *IEEE Trans. Autom. Control*, **52**(4):736–742, 2007, <https://doi.org/10.1109/TAC.2007.894543>.
6. B. Cui, X. Lou, Synchronization of chaotic recurrent neural networks with time-varying delays using nonlinear feedback control, *Chaos Solitons Fractals*, **39**(1):288–294, 2009, <https://doi.org/10.1016/j.chaos.2007.01.100>.
7. Q. Gan, Exponential synchronization of stochastic Cohen-Grossberg neural networks with mixed time-varying delays and reaction-diffusion via periodically intermittent control, *Neural Netw.*, **31**:12–21, 2012, <https://doi.org/10.1016/j.neunet.2012.02.039>.
8. K. Gopalsamy, X. He, Stability in asymmetric Hopfield nets with transmission delays, *Physica D*, **76**(4):344–358, 1994, [https://doi.org/10.1016/0167-2789\(94\)90043-4](https://doi.org/10.1016/0167-2789(94)90043-4).
9. J. Hale, *Introduction to Functional Differential Equations*, Springer, New York, 1993, <https://doi.org/10.1007/978-1-4612-4342-7>.
10. J. Hopfield, Neural networks and physical systems with emergent collective computational abilities, *Proc. Natl. Acad. Sci. USA*, **79**:2254–2258, 1982, <https://doi.org/10.1073/pnas.79.8.2554>.
11. C. Hu, J. Yu, H. Jiang, Z. Teng, Exponential synchronization for reaction-diffusion networks with mixed delays in terms of p-norm via intermittent driving, *Neural Netw.*, **31**:1–11, 2012, <https://doi.org/10.1016/j.neunet.2012.02.038>.
12. R. Kumar, S. Das, Y. Cao, Effects of infinite occurrence of hybrid impulses with quasi-synchronization of parameter mismatched neural networks, *Neural Netw.*, **122**:106–116, 2020, <https://doi.org/10.1016/j.neunet.2019.10.007>.
13. L. Levaggi, Infinite dimensional systems sliding motions, *Eur. J. Control*, **8**(6):508–516, 2002, <https://doi.org/10.3166/ejc.8.508-516>.
14. X. Liang, L. Wang, Y. Wang, R. Wang, Dynamical behavior of delayed reaction-diffusion Hopfield neural networks driven by infinite dimensional Wiener processes, *IEEE Trans. Neural Networks Learn. Syst.*, **27**(8):1231–1242, 2016, <https://doi.org/10.1109/TNNLS.2015.2460117>.

15. X. Liang, R. Wang, R. Ghanem, Uncertainty quantification of detonation through adapted polynomial chaos, *Int. J. Uncertain. Quantif.*, **10**(1):83–100, 2020, <https://doi.org/10.1109/9.855545>.
16. X. Liao, S. Yang, S. Cheng, Y. Shen, Stability of generalized neural networks with reaction-diffusion terms, *Sci. Chin., Ser. F*, **44**(5):389–395, 2001 (in Chinese??).
17. X. Liu, K. Zhang, W. Xie, Pinning impulsive synchronization of reaction-diffusion neural networks with time-varying delays, *IEEE Trans. Neural Networks Learn. Syst.*, **28**(5):1055–1067, 2017, <https://doi.org/10.1109/TNNLS.2016.2518479>.
18. B. Lu, H. Jiang, C. Hu, A. Abdurahman, Synchronization of hybrid coupled reaction-diffusion neural networks with time delays via generalized intermittent control with spacial sampled-data, *Neural Netw.*, **105**:75–87, 2018, <https://doi.org/10.1016/j.neunet.2018.04.017>.
19. Q. Luo, F. Deng, J. Bao, B. Zhao, Sliding mode control for a class of Itô type distributed parameter systems with delay, *Acta Math. Sci.*, **27**(1):67–76, 2007, [https://doi.org/10.1016/S0252-9602\(07\)60006-x](https://doi.org/10.1016/S0252-9602(07)60006-x).
20. H. Lutkepohl, *Handbook of Matrices*, John Wiley & Sons, New York, 1996, <https://doi.org/04719668860471970158>.
21. C. Marcus, R. Westervelt, Stability of analog neural networks with delay, *Phys. Rev. A*, **39**(3):347–359, 1989, <https://doi.org/10.1103/PhysRevA.39.347>.
22. A. Michel, D. Liu, *Qualitative Analysis and Synthesis of Recurrent Neural Networks*, Marcel Dekker, New York, 2002, <https://doi.org/10.1201/9781482275780>.
23. Y. Niu, D. Ho, X. Wang, Sliding mode control for Itô stochastic systems with Markovian switching, *Automatica*, **43**(10):1784–1790, 2007, <https://doi.org/10.1016/j.automatica.2007.02.023>.
24. Y. Orlov, Discontinuous unit feedback control of uncertain infinite dimensional systems, *IEEE Trans. Autom. Control*, **45**(5):834–843, 2000, <https://doi.org/10.1109/9.855545>.
25. Y. Orlov, V. Utkin, Sliding mode control in indefinite dimensional systems, *Automatica*, **23**(6):753–757, 1987, [https://doi.org/10.1016/0005-1098\(87\)90032-X](https://doi.org/10.1016/0005-1098(87)90032-X).
26. L. Pecora, T. Carroll, Synchronization in chaotic systems, *Phys. Rev. Lett.*, **64**(8):821–824, 1990, <https://doi.org/10.1142/S0218127496000965>.
27. T. Roska, C.W. Wu, M. Balsa, L.O. Chua, Stability and dynamics of delay-type general and cellular neural networks, *IEEE Trans. Circuits Syst., I, Fundam. Theory Appl.*, **39**(6):487–490, 1992, <https://doi.org/10.1109/81.153647>.
28. Q. Song, Z. Wang, Neural networks with discrete and distributed time-varying delays: A general stability analysis, *Chaos Solitons Fractals*, **37**(5):1538–1547, 2008, <https://doi.org/10.1016/j.chaos.2006.10.044>.
29. H. Wang, G. Feng, Synchronization of nonidentical chaotic neural networks with time delays, *Neural Netw.*, **22**(7):869–874, 2009, <https://doi.org/10.1016/j.neunet.2009.06.009>.
30. J. Wang, H. Wu, T. Huang et al, Pinning control strategies for synchronization of linearly coupled neural networks with reaction-diffusion terms, *IEEE Trans. Neural Networks Learn. Syst.*, **27**(4):749–761, 2016, <https://doi.org/10.1109/TNNLS.2015.2423853>.

31. Q. Wang, Computation issue of pointwise controls for diffusion Hopfield neural network system, *Appl. Math. Comput.*, **207**(1):267–275, 2005, <https://doi.org/10.1016/j.amc.2008.10.043>.
32. T. Wei, P. Lin, Y. Yang, L. Wang, Stability of stochastic impulsive reaction-diffusion neural networks with s-type distributed delays and its application to image encryption, *Neural Netw.*, **116**:35–45, 2019, <https://doi.org/10.1016/j.neunet.2019.03.016>.
33. L. Wu, D. Ho, Sliding mode control of singular stochastic hybrid systems, *Automatica*, **46**(2):779–783, 2010, <https://doi.org/10.1016/j.automatica.2010.01.010>.
34. H. Xing, C. Gao, D. Li, Sliding mode variable structure control for parameter uncertain stochastic systems with time-varying delay, *J. Math. Anal. Appl.*, **35**(2):689–699, 2009, <https://doi.org/10.1109/RAMECH.2008.4681341>.
35. T. Yang, L. Chua, Impulsive stabilization for control and synchronization of chaotic system: Theory and application to secure communication, *IEEE Trans. Circuits Syst., I, Fundam. Theory Appl.*, **44**(10):976–988, 1997, <https://doi.org/10.1109/81.633887>.
36. X. Yang, J. Cao, J. Liang, Exponential synchronization of memristive neural networks with delays: Interval matrix method, *IEEE Trans. Neural Networks Learn. Syst.*, **28**(8):1878–1888, 2017, <https://doi.org/10.1109/TNNLS.2016.2561298>.
37. X. Yang, X. Li, J. Lu, Z. Cheng, Synchronization of time-delayed complex networks with switching topology via hybrid actuator fault and impulsive effects control, *IEEE Trans. Cybern.*, **50**(9):4043–4052, 2020, <https://doi.org/10.1109/TCYB.2019.2938217>.
38. X. Yang, Y. Liu, J. Cao, L. Rutkowski, Synchronization of coupled time-delay neural networks with mode-dependent average dwell time switching, *IEEE Trans. Neural Networks Learn. Syst.*, **31**(12):5483–5496, 2020, <https://doi.org/10.1109/TNNLS.2020.2968342>.
39. X. Yang, Y. Liu, J. Cao, L. Rutkowski, Synchronization of switched discrete-time neural networks via quantized output control with actuator fault, *IEEE Trans. Neural Networks Learn. Syst.*, 2020, <https://doi.org/10.1109/TNNLS.2020.3017171>.
40. X. Yang, Q. Song, J. Cao, J. Lu, Synchronization coupled Markovian reaction-diffusion neural networks with proportional delays via quantized control, *IEEE Trans. Neural Networks Learn. Syst.*, **30**(3):951–958, 2019, <https://doi.org/10.1109/TNNLS.2018.2853650>.
41. Z. Zhang, J. Wang, Novel finite-time synchronization criteria for inertial neural networks with time delays via integral inequality method, *IEEE Trans. Neural Networks Learn. Syst.*, **30**(5):1476–1485, 2019, <https://doi.org/10.1109/TNNLS.2020.3017171>.
42. Q. Zhu, J. Cao, Stability of Markovian jump neural networks with impulse control and time varying delays, *Nonlinear Anal., Real World Appl.*, **13**(5):2259–2270, 2012, <https://doi.org/10.1016/j.nonrwa.2012.01.021>.